Functional characterization of thioesterase superfamily member 1/Acyl-CoA thioesterase 11: implications for metabolic regulation[S]

Shuxin Han and David E. Cohen[1]

Department of Medicine, Division of Gastroenterology, Brigham and Women's Hospital,
Harvard Medical School, Boston, MA 02115

Abstract Thioesterase superfamily member 1 (Them1; synonyms acyl-CoA thioesterase 11 and StarD14) is highly expressed in brown adipose tissue and limits energy expenditure in mice. Them1 is a putative fatty acyl-CoA thioesterase that comprises tandem hot dog-fold thioesterase domains and a lipid-binding C-terminal steroidogenic acute regulatory protein-related lipid transfer (START) domain. To better define its role in metabolic regulation, this study examined the biochemical and enzymatic properties of Them1. Purified recombinant Them1 dimerized in solution to form an active fatty acyl-CoA thioesterase. Dimerization was induced by fatty acyl-CoAs, coenzyme A (CoASH), ATP, and ADP. Them1 hydrolyzed a range of fatty acyl-CoAs but exhibited a relative preference for long-chain molecular species. Thioesterase activity varied inversely with temperature, was stimulated by ATP, and was inhibited by ADP and CoASH. Whereas the thioesterase domains of Them1 alone were sufficient to yield active recombinant protein, the START domain was required for optimal enzyme activity.[S] An analysis of subcellular fractions from mouse brown adipose tissue and liver revealed that Them1 contributes principally to the fatty acyl-CoA thioesterase activity of microsomes and nuclei. These findings suggest that under biological conditions, Them1 functions as a lipid-regulated fatty acyl-CoA thioesterase that could be targeted for the management of metabolic disorders.—Han, S., and D. E. Cohen. **Functional characterization of thioesterase superfamily member 1/Acyl-CoA thioesterase 11: implications for metabolic regulation.** *J. Lipid Res.* 2012. 53: 2620–2631.

Supplementary key words long-chain fatty acyl-CoA • free fatty acid • brown adipose tissue • liver • recombinant protein • START domain

Members of the acyl-CoA thioesterase (Acot) gene family hydrolyze acyl-CoA molecules. Substrates of these enzymes include a variety of coenzyme A (CoASH) thioesters, including fatty acyl- and acetyl-CoAs (1, 2). Although their biological functions remain largely undefined, it has been postulated that Acots may control the intracellular balance of fatty acyl-CoA and free fatty acids, regulate concentrations of CoASH, and liberate fatty acids for the biosynthesis of inflammatory mediators (1, 2). Thirteen mammalian Acot genes are divided into two types, which differ according to the structural organization of the catalytic domains: type I enzymes (Acots 1–6) contain an α/β-hydrolase domain, whereas type II enzymes (Acots 7–13) comprise one or two hot dog-like thioesterase domains (1). Acots have been identified in a broad array of organisms and exhibit differential tissue distributions and subcellular localizations. Recent studies in mice have linked Acots to nutrient metabolism and energy homeostasis (3, 4).

Acot11, more commonly referred to as thioesterase superfamily member 1 (Them1), and Acot12, also known as cytosolic acetyl-CoA hydrolase, are unique among Acot family members because they contain a C-terminal steroidogenic acute regulatory transfer-related (START) domain in addition to the tandem N-terminal hot dog-fold domains. Consequently, Them1 and Acot12 are classified as StarD14 and StarD15, respectively, within the START domain gene family (5). START domains share a similar three-dimensional conformation, including a helix-grip fold that forms a hydrophobic tunnel to accommodate a lipid molecule, and have been postulated to play key roles in lipid sensing, lipid transfer, and signaling (6). Although START domains generally reside at the C terminus of multidomain proteins such as Them1 and Acot12, they also exist as single-domain proteins, which are referred to as "START domain minimal proteins." In earlier studies (7, 8), we demonstrated that the

---

Abbreviations: Acot, acyl-CoA thioesterase; ATP-γ-S, adenosine 5′-[γ-thio]triphosphate; BAT, brown adipose tissue; BFIT, brown fat-inducible thioesterase; CMC, critical micellar concentration; CoASH, coenzyme A; GST, glutathione S-transferase; PC-TP, phosphatidylcholine transfer protein; START, steroidogenic acute regulatory protein-related lipid transfer, also recombinant protein containing the START domain of Them1; Them, thioesterase superfamily member; Thio1, recombinant protein containing N-terminal thioesterase domain of Them1; Thio1/2, recombinant protein containing both thioesterase domains of Them1.

[1] To whom correspondence should be addressed.
e-mail: dcohen@partners.org

[S] The online version of this article (available at http://www.jlr.org) contains supplementary data in the form of one table and five figures.

START domain minimal protein phosphatidylcholine transfer protein (PC-TP, synonym StarD2) binds to Them2 (synonym for Acot13) and increases the rate of hydrolysis of long-chain fatty acyl-CoAs.

Them1 is highly expressed in brown adipose tissue (BAT) and was initially named brown fat-inducible thioesterase (BFIT) because it was strongly up-regulated by decreases in ambient temperature (9). When taken together with the observation that Them1 gene expression was higher in BAT of mouse strains that were resistant to diet-induced obesity, it was predicted that Them1 functioned to promote energy expenditure. However, we recently demonstrated that energy expenditure was increased in $Them1^{-/-}$ mice, which were highly resistant to diet-induced obesity, as well as associated metabolic disorders (4).

Although increased BAT concentrations of fatty acyl-CoAs and decreased thioesterase activities of BAT homogenates suggested that Them1 functions as an Acot in vivo (4), the enzymatic characteristics of mouse Them1 and the two alternatively spliced isoforms of human THEM1, herein referred to as THEM1a (synonym BFIT1) and THEM1b (synonym BFIT2), remain unknown. The current study was designed to systematically explore key properties of purified recombinant Them1/THEM1 and to correlate these with measurements of acyl-CoA thioesterase activity in subcellular fractions of BAT and liver from $Them1^{+/+}$ and $Them1^{-/-}$ mice. Our results demonstrate that Them1 forms a homodimer that preferentially hydrolyzes long-chain fatty acyl-CoAs and that the START domain contributes toward optimizing this activity.

MATERIALS AND METHODS

Reagents

Acyl-CoA thioesters, myristic acid, ATP, the nonhydrolyzable ATP analog adenosine 5′-[γ-thio]triphosphate (ATP-γ-S), ADP, CoASH, and 5,5′-dithiobis-(2-nitrobenzoic acid) were purchased from Sigma-Aldrich (St. Louis, MO). The plasmid pCMV-SPORT6-Them1 was obtained from Invitrogen (Grand Island, NY), pCMV6-XL5-BFIT1 was from OriGene (Rockville, MD), pGEX-KG was from Lablife (Northfield, MN), and pCR4-TOPO-BFIT2 and pCR4-TOPO-Acot12 were from Open Biosystems (Lafayette, CO). A glutathione S-transferase (GST)-PCTP expression plasmid (pGEX-KG-PCTP) was as described (10). Phusion High-Fidelity DNA Polymerase was from Thermo Scientific (Waltham, MA).

Molecular cloning

The open reading frames of full-length and truncated Them1, THEM1a, THEM1b, and Acot12 were amplified using PCR based on template plasmids, digested with restriction enzymes, and cloned into the expression vector pGEX-KG according to supplementary Table I.

Expression and purification of recombinant proteins

Expression plasmids were transformed into the *Escherichia coli* strain BL21 (DE3). Bacteria were grown in LB, and protein expression was induced using 2 mM isopropyl β-D-thiogalactopyranoside followed by shaking at 23°C for 24–72 h. Bacteria were pelleted by centrifugation and lysed using 25 mM Tris-HCl (pH 7.5), 100 mM NaCl, 2 mM EDTA, and 0.5% Triton X-100 plus protease inhibitors (Protease Inhibitor Cocktail Tablets; Roche, Basel, Switzerland). Lysates were sonicated 6×10 s (Fisher Sonic Dismembrator Model 300; Fisher Scientific, Pittsburgh, PA),

rotated at 4°C for 1 h, and centrifuged at 11,000 g for 20 min. If not used immediately, supernatants were frozen at −80°C. GST fusion proteins were purified by FPLC using a GST affinity column (GSTrap HP column; GE Healthcare, Waukesha, WI). Briefly, lysates were applied to the column after equilibration with 140 mM NaCl, 2.7 mM KCl, 10 mM Na$_2$HPO$_4$, and 1.8 mM KH$_2$PO$_4$ (pH 7.3) and then washed with 5 column volumes of the same buffer. GST-fusion proteins were eluted using 10 mM reduced glutathione (50 mM Tris-HCl at pH 8.0). In some experiments, GST fusion proteins were purified by incubating clarified bacterial lysates with glutathione-coated beads (GE Healthcare). The beads were rotated at 4°C for at least 6 h before pelleting at 1,300 g for 2 min. Beads were then washed three times with cold PBS, and GST fusion proteins were eluted using the same elution buffer as described for FPLC purification. GST-fusion proteins were further purified by FPLC using a 16 mm × 60 cm Superdex 75 gel filtration column (GE Healthcare) equilibrated with 50 mM NaH$_2$PO$_4$ and 150 mM NaCl (pH 7.2). The purified protein was concentrated using Amicon Ultra-15 Centrifugal Filter Units (Millipore, Billerica, MA). To cleave the GST tag, thrombin (1 unit/µl; GE Healthcare) was mixed with GST-fusion proteins (100 µg/unit) and incubated at 23°C for at least 16 h. After 6 h rotation at 4°C, glutathione-coated beads (GE Healthcare) were added to pellet the GST tag. Thrombin was used to cleave proteins while still bound to GST beads by incubation at 23°C for at least 16 h. Beads were then pelleted, leaving the untagged protein in the supernatant. Protein purities were assessed using SDS-PAGE gel and Coomassie Brilliant Blue staining. Protein concentrations were determined by using the molar absorption coefficient at 280 nm, which was calculated based on the primary sequence, or by using the Bradford method (8). Protein samples were used immediately or stored at −80°C.

Protein oligomerization

Oligomerization was determined by FPLC using a Superose 6 10/300 GL column (GE Healthcare). The column was pre-equilibrated with the 50 mM NaH$_2$PO$_4$ and 150 mM NaCl (pH 7.2) before application of purified proteins (400 µl of 5 µM solutions). Proteins were eluted with the same buffer at a flow rate of 0.5 ml/min at 23°C or 4°C. After collection in glass test tubes, fractions (300 µl) were transferred to individual wells of a 96-well UV plate (Fisher Scientific). Relative protein concentrations were determined by A_{280} using a SpectraMax M5 microplate reader (Molecular Devices, Sunnyvale, CA). The column was calibrated using a Gel Filtration Calibration Kit HMW (GE Healthcare), which allowed the determination of apparent molecular weights for recombinant proteins. To examine chemical effects on protein oligomerization, recombinant proteins were incubated with ATP (2 mM), ATP-γ-S (0.5 mM), ADP (0.5 mM), palmitoyl-CoA (25 µM), acetyl-CoA (50 µM), CoASH (50 µM), or myristic acid (25 µM) for 30 min at 23°C or 37°C. To insure its solubility at the concentrations used in this and subsequent experiments (11), myristic acid was first converted to its potassium salt using methanolic KOH and then dried under a stream of nitrogen before being dissolved in aqueous buffer. Before FPLC, samples were ultrafiltered using a 10 kDa MWCO Microcon Centrifugal Filter Devices (Millipore) at 11,000 g for 40 min.

Acyl-CoA thioesterase activity assay

The acyl-CoA thioesterase activity of purified recombinant protein or tissue extracts was determined as previously described (8). Briefly, an acyl-CoA substrate was mixed in 50 mM KCl, 10 mM Hepes (pH 7.5), and 0.3 mM 5,5′-dithiobis-(2-nitrobenzoic acid) in 96-well plates (Fisher Scientific). Protein was added to initiate acyl-CoA hydrolysis in a total reaction volume of 200 µl/well. Plates were immediately introduced into a temperature-controlled SpectraMax M5 microplate reader and mixed for 5 s. Absorbance readings at 412 nm (A_{412}) were read at 1 min intervals at 37°C for 60 min.

Kinetic characterization of acyl-CoA thioesterase activity

Steady-state kinetic parameters were determined as previously described (8). Briefly, acyl-CoA thioesterase activities were determined as functions of time after mixing of the enzyme (E) with the substrate (S) acyl-CoA. Initial rates (V_0) were determined using SoftMax Pro software (Molecular Devices). Values of [S] were varied to create saturation curves, and values of V_0 were fitted to the Michaelis–Menten equation, $V_0 = V_{max}[S]/([S] + K_m)$, using Prism 5 (GraphPad Software Inc., La Jolla, CA) to yield V_{max} (the maximum rate) and K_m (the Michaelis constant). We found that nonlinear analysis of the Michealis-Menten equation provided satisfactory curve-fits, with an average $R^2 = 0.99$ and a minimum $R^2 > 0.95$. In some experiments, values of K_m and V_{max} were determined by linear analysis of Lineweaver-Burk plots. Values of k_{cat} were calculated as $k_{cat} = V_{max}/[E]$.

Subcellular fractionation of mouse tissues

Male $Them1^{+/+}$ and $Them1^{-/-}$ mice were bred and maintained as described (4). Mice ranging from 8–16 weeks of age were euthanized, and tissues were harvested for immediate use or storage at −80°C. Isolated mouse brown adipose tissue (BAT) and livers were rinsed three times in ice-cold PBS. Tissues were gently homogenized for 2 min in nondenaturing lysis buffer containing 20 mM Tris (pH 8.0), 137 mM NaCl, 1 mM EDTA, 10% glycerol, and 0.5% Triton X-100. Homogenates were then sonicated for 4×10 s pulses (Fisher Sonic Dismembrator Model 300) and rotated at 4°C for 30 min. After centrifugation at 16,000 g for 10 min, the supernatants were transferred to new Eppendorf tubes without disturbing the floating fat layer. For BAT, this centrifugation step was repeated for four times to eliminate fat. The isolation of nuclei, mitochondria, microsomes, and cytosol was as described (12), with purities as previously demonstrated (see supplementary Fig. S1B in Reference 4). Isolated nuclei, mitochondria, and microsomes were resuspended using the same nondenaturing buffer described as above. Lysates were prepared by sonication and rotated at 4°C for 30 min. Samples were centrifuged at 1,300 g for 5 min, and the supernatants were transferred to new Eppendorf tubes. Protein concentrations were determined by the Bradford method. Samples were stored at −80°C for later use. Protocols for animal use were approved by the institutional committee of Harvard Medical School.

Immunofluorescence and immunohistochemistry

A polyclonal antibody raised to the Them1 peptide PQKLPWIR-PQPGEGERRY (4) was affinity purified first using this peptide and then again using the truncated peptide PQPGEGERRY to eliminate residual nonspecific binding. Excised tissues were fixed in formalin and embedded in paraffin before sectioning. Tissue sections were deparaffinized and rehydrated before heat-mediated antigen retrieval with sodium citrate buffer (10 mM, pH 6.0). For immunofluorescence microscopy of BAT, background autofluorescence was quenched by incubation with sodium borohydride (1 mg/ml) at room temperature for 5 min. After washing the sections with water and TBS, tissues were blocked with 5% normal donkey serum at room temperature for 1 h. Sections were then incubated overnight at 4°C with a 1:50 dilution of the affinity-purified anti-Them1 antibody. Sections were washed with TBS and incubated with Dylight 649-conjugated donkey anti-rabbit secondary antibody (1:200; Jackson ImmunoResearch Laboratories, West Grove, PA) at room temperature for 1.5 h. After rinsing the sections in TBS, the slides were mounted with Prolong Gold Anti-fade mounting media (Invitrogen) and stained with Hoechst 33342 (Invitrogen). Confocal images were taken using a Zeiss LSM510 Meta confocal system with Zeiss LSM510 image acquisition software (Carl Zeiss, Thornwood, NY). Images were acquired using 20×/0.8

Plan-Apochromat and 63×/N.A. 1.3 Oil Plan-Apochromat objectives (Carl Zeiss). For immunohistochemistry, background peroxidase activity was quenched by incubation with 3% H_2O_2 at room temperature for 10 min. After washing the sections with water and TBS, tissues were blocked with an Avidin/Biotin Blocking Kit (SP2001; Vector Laboratories, Burlingame, CA). After the same blocking and primary antibody treatment as described for immunofluorescence, sections were washed with TBS and incubated with biotin-conjugated donkey anti-rabbit secondary antibody (1:400; Jackson ImmunoResearch Laboratories) at room temperature for 1.5 h. Sections were then rinsed in TBS, enhanced with Vectastain ABC Kit (PK-6100; Vector Laboratories), and developed with DAB Reagent (SK-4100; Vector Laboratories) for 40 s. The tissue was counterstained with hematoxylin and mounted with Permount. Slides were imaged and photographed using a Zeiss Axio-imager M1 microscope (Carl Zeiss) using the same objectives as for immunofluorescence and AxioVision 4.6 software.

Statistical analysis

Data are presented as means ± SEM and were analyzed for statistical significance using a two-tailed unpaired Student's t-test using Prism 5 (GraphPad Software).

RESULTS

Design of recombinant proteins

Fig. 1A illustrates the protein constructs that we used to characterize thioesterase activities. We prepared purified recombinant proteins that included full-length Them1, THEM1a, THEM1b, and Acot12 as well as the following truncation mutants: N-terminal thioesterase domain of Them1 (Thio1), both thioesterase domains (Thio1/2), the START domain of Them1, and PC-TP. Fig. 1B demonstrates the purification of GST-Them1 using GST affinity chromatography followed by size exclusion chromatography, after which the GST tag was removed enzymatically, as confirmed by SDS-PAGE.

We initially compared the thioesterase activity of GST-Them1 and Them1 using long-chain fatty acyl-CoAs (i.e., myristoyl-CoA, palmitoyl-CoA, and stearoyl-CoA).[2] Fig. 1C

---

[2] Each of these acyl-CoAs is soluble at concentrations ranging up to 25 μM. At room temperature, the aqueous solubility of myristoyl-CoA exceeds 200 μM (13). The solubilities of palmitoyl-CoA and stearoyl-CoA are in excess of 140 μM and 45 μM, respectively, at room temperature (14). Because substrate inhibition of Acots occurs when acyl-CoA concentrations reach their critical micelle concentration (CMC) values (summarized in Reference 8), we also took care to use submicellar concentrations to characterize enzyme activity in these studies. At room temperature, reported CMC values are 210 μM for myristoyl-CoA (13) and range from 30 to 80 μM for palmitoyl-CoA (13–16). As a result, myristoyl-CoA and palmitoyl-CoA were monomeric substrates in the kinetic experiments performed at 23°C in our study (see Figure 5). Most of our kinetic experiments were performed at 37°C, with a few at 45°C (see Figure 5). Because increases in temperature lead to substantial increases in solubilities and CMC values (8, 14), myristoyl-CoA and palmitoyl-CoA in these studies were monomeric. This was also most likely the case for stearoyl-CoA, which exhibits a CMC of 7.5–12 μM at room temperature (13, 14) but was studied by us at 37°C. Although the CMC value for stearoyl-CoA at 37°C has not been reported, only the highest concentration of stearoyl-CoA we used (25 μM) fell substantially above the reported range of room-temperature CMCs. Considering that the CMC value for stearoyl-CoA should be considerably higher at 37°C and that the V_0 value for Them1 at 25 μM was consistent with values observed at lower monomeric substrate concentrations, it is very unlikely that substrate inhibition occurred for stearoyl-CoA.

A

B

C
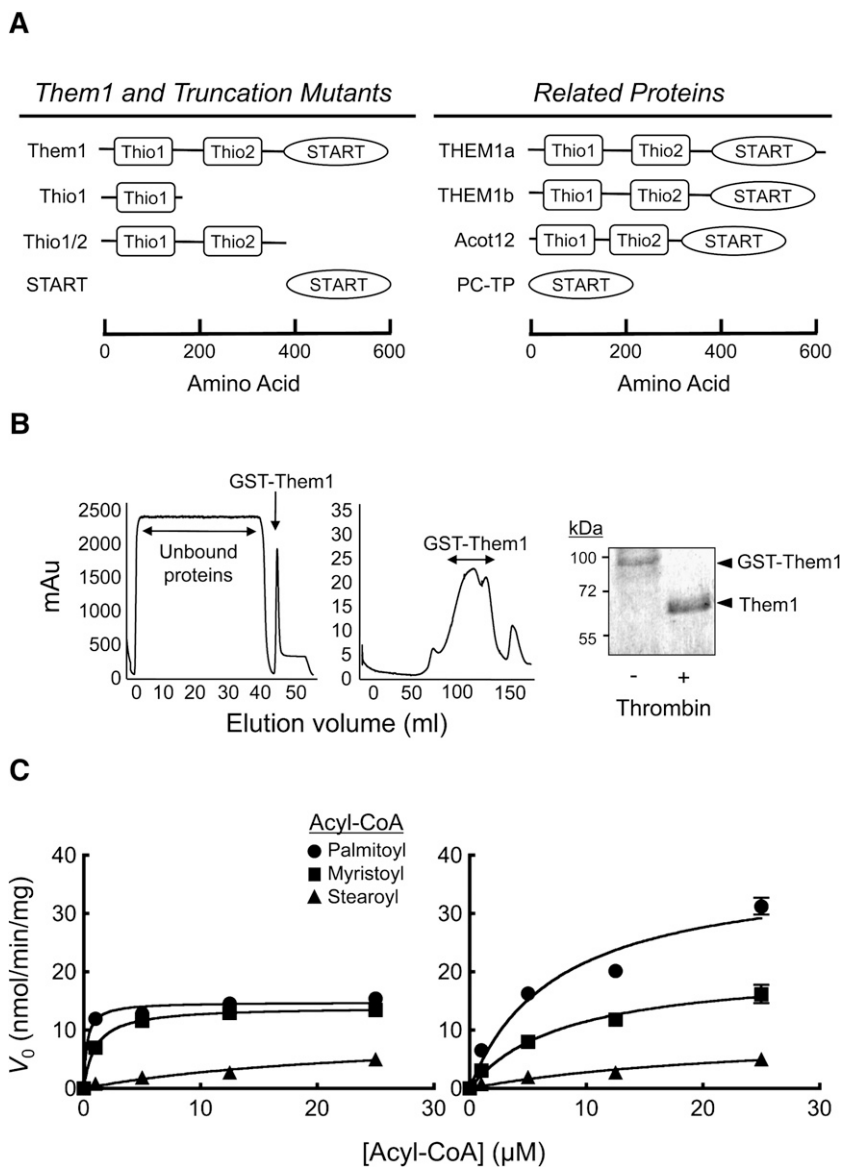
Fig. 1. Design, purification, and activities of recombinant proteins. A: Schematic diagram of recombinant proteins used in this study. Full-length proteins were Them1 (aa 1–594), THEM1a (aa 1–607), THEM1b (aa 1–594), Acot12 (aa 1–556), and PC-TP (aa 1–214). Truncation mutations of Them1 were Thio1 (aa 1–167), Thio1/2 (aa 1–379), and START (aa 380–594). B: Purification of recombinant Them1. Recombinant expressed GST-Them1 was first subjected to GST affinity chromatography (left panel). After washing unbound proteins, GST-Them1 was eluted using reduced glutathione. GST-Them1 was further purified by size exclusion chromatography (center panel). The GST tag was cleaved using thrombin to obtain Them1, as verified by SDS-PAGE (right panel). C: Thioesterase activity of GST-Them1 and Them1. Saturation curves of initial velocity (V_0) at 37°C are shown for GST-Them1 (left panel) and Them1 (right panel) using three long-chain fatty acyl-CoAs. Solid lines indicate fit of the data to the Michaelis-Menten equation. Where not visible, error bars are contained within the symbol sizes.

shows that the enzymatic activities of Them1 before (left panel) and after (right panel) removal of the GST tag. GST-Them1 demonstrated thioesterase activity using all three substrates but most efficiently hydrolyzed palmitoyl-CoA. Removal of the GST tag from Them1 increased the K_m (µM) and V_{max} (nmol/min/mg) values of Them1 for palmitoyl-CoA (K_m: GST-Them1 0.3 ± 0.02, Them1 7.5 ± 0.5; V_{max}: GST-Them1 14.8 ± 0.6, Them1 38.1 ± 1.8) and myristoyl-CoA (K_m: GST-Them1 1.0 ± 0.2, Them1 8.1 ± 0.9; V_{max}: GST-Them1 14 ± 0.5, Them1 20.9 ± 1.7) but not stearoyl-CoA (K_m: GST-Them1 28.6 ± 6.9, Them1

28.0 ± 4.8; V_{max}: GST-Them1 10.3 ± 1.3, Them1 10.3 ± 0.8). On this basis, the GST was removed in subsequent experiments.

Oligomerization of Them1

We next used FPLC to examine whether Them1 forms oligomers and to determine the conditions that influence oligomerization (**Fig. 2**). At 23°C and 4°C, Them1 eluted principally at a molecular weight of 67 kDa, which is consistent with a monomer (Fig. 2A). At 4°C, there was a small second peak associated with the main peak
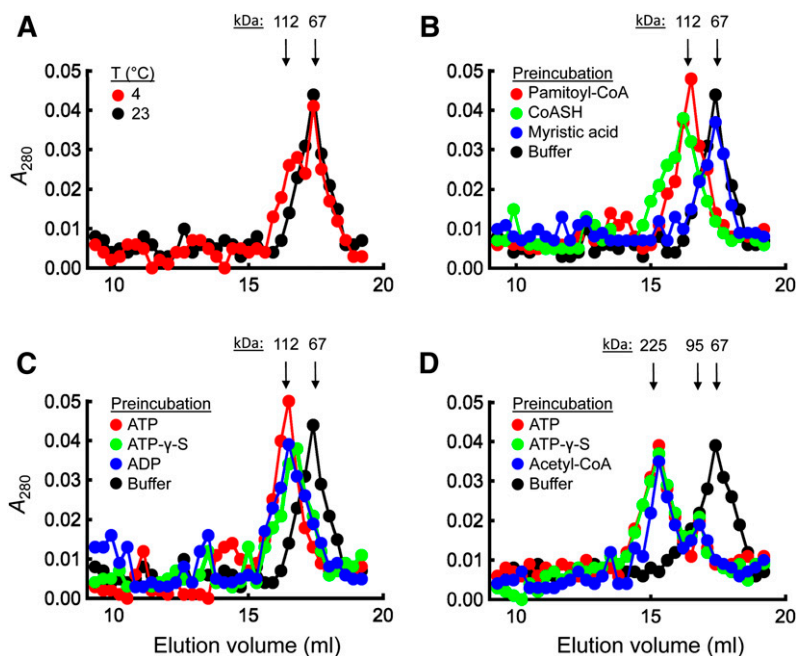
Fig. 2. Oligomerization of Them1. A: FPLC elution profile showing that purified recombinant Them1 existed principally as a monomer in solution at 4°C and 23°C. B: The influence of substrate and products on Them1 dimerization was determined by incubating Them1 with palmitoyl-CoA (25 µM), CoASH (50 µM), myristic acid (25 µM), or column buffer at 23°C for 30 min before FPLC. C: The effects of ATP, an analog, and its metabolite on Them1 dimerization were determined by preincubating Them1 with ATP (2 mM), ATP-γ-S (0.5 mM), ADP (0.5 mM), or column buffer at 23°C for 30 min. D: FPLC elution profile of purified recombinant Acot12 after preincubation with ATP (2 mM), ATP-γ-S (0.5 mM), acetyl-CoA (50 µM), or column buffer at 23°C for 30 min.

that corresponded to an apparent molecular weight of 112 kDa and suggested the potential presence of dimers. Upon incubation with palmitoyl-CoA, the elution volume for the entire Them1 protein peak corresponded to an apparent molecular weight of 112 kDa (Fig. 2B), indicative of a Them1 dimer. The same effect was induced by preincubation of Them1 with CoASH but not by myristic acid. Because ATP has been shown to induce tetramerization of Acot12 (17), we tested its effects on Them1. When Them1 was preincubated with ATP (Fig. 2C), we again observed a decrease in elution volume, suggestive of dimerization. The same effect was also observed in the presence ATP-γ-S and ADP. In keeping with the observation that it exists as monomer or dimer in the absence of ATP (17), the elution profile of Acot12 under the current experimental conditions (Fig. 2D) was indicative of a monomer with a molecular weight of 67 kDa. A leading shoulder associated with this peak was consistent with a dimer fraction. After incubation with ATP, ATP-γ-S, or acetyl-CoA, the elution volume of Acot12 corresponded primarily to an apparent molecular weight of 225 kDa, consistent with a tetramer, but also a smaller peak of 95 kDa apparent molecular weight, consistent with a dimer (17).
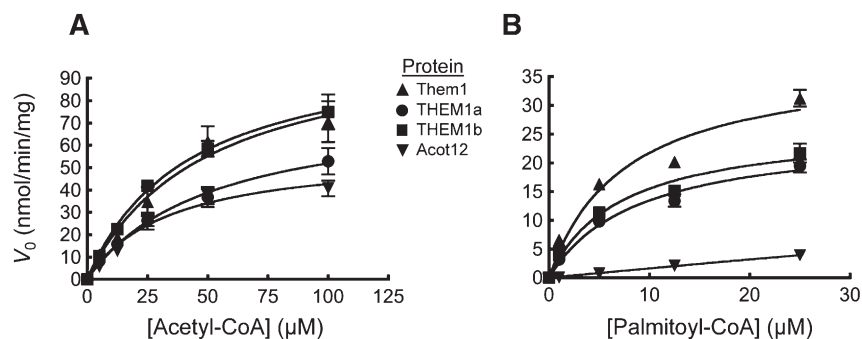
Substrate specificities

We next examined the thioesterase activities of Them1 and of THEM1a and THEM1b using acetyl-CoA (**Fig. 3A**) and palmitoyl-CoA (Fig. 3B) as substrates. Acot12, Them1, THEM1a, and THEM1b each hydrolyzed acetyl-CoA molecules, with values of K_m and V_{max} (**Table 1**) for Them1, THEM1a, and THEM1b that were each somewhat higher than for Acot12 (K_m = 34.1 ± 2.1 µM; V_{max} = 57.2 ± 4.4 nmol/min/mg). As was the case for Them1, THEM1a and THEM1b exhibited robust thioesterase activity toward palmitoyl-CoA, with similar K_m values for each but with Them1 exhibiting a higher value of V_{max} compared with THEM1a and THEM1b (Table 1). However, as has been

previously reported (18), Acot12 had no appreciable palmitoyl-CoA thioesterase activity (Fig. 3B). Table 1 also lists for Them1 the steady-state enzymatic constants for a variety of acyl-CoA molecular species. These data reveal that Them1 is capable of catalyzing a broad range of acyl-CoA molecules, although the lowest K_m values were observed for long- and medium-chain fatty acyl-CoAs and the highest values of k_{cat}/K_m were for palmitoyl-CoA, myristoyl-CoA, and lauroyl-CoA.

Fig. 4 shows the effects of selected small molecules on the acyl-CoA thioesterase activity of Them1 using palmitoyl-CoA as the substrate. To ensure that differences in steady-state kinetic constants were not influenced by the method of analysis and to gain insights into molecular mechanisms of Them1 regulation, the data in this experiment were analyzed by nonlinear analysis of the Michaelis-Menten equation (Fig. 4A, left panel) and linear analysis of Lineweaver-Burke plots (Fig. 4A, right panel). Fig. 4B shows that there was good concordance between the two analyses ($R^2 \geqslant 0.98$) for each steady-state kinetic constant, with slope values within 11% of unity and intercept values that were close to 0. The presence of myristic acid had no effect on the activity of Them1. As evidenced by decreases in K_m along with increases in V_{max}, k_{cat}, and k_{cat}/K_m, Them1 activity was increased by ATP and ATP-γ-S (Fig. 4B). Conversely, activity was decreased by the addition of ADP and CoASH. The intersection of regression lines between the vertical and horizontal axis of the Lineweaver-Burk plots (Fig. 4A, right panel) indicated that inhibition of Them1 was by a mixed mechanism for these two compounds.

Effect of temperature on Them1 activity

We next measured the temperature dependence of Them1 activity using palmitoyl-CoA (**Fig. 5A**) and myristoyl-CoA (Fig. 5B) as substrates. For both substrates, values of K_m decreased as functions of decreasing temperatures (Fig. 5C), whereas V_{max} increased for palmitoyl-CoA and myristoyl-CoA

Fig. 3. Acyl-CoA substrate specificities of full-length recombinant proteins. Saturation curves of V_0 for Them1, THEM1a, THEM1b, or Acot12 at 37°C using acetyl-CoA (A) or palmitoyl-CoA (B) as substrates. Solid lines indicate fit of the data to the Michaelis-Menten equation. Where not visible, error bars are contained within the symbol sizes.

(Fig. 5D). These changes yielded decreases in k_{cat} (Fig. 5E) but much sharper decreases in k_{cat}/K_m for Them1 as the temperature was increased from 23°C to 37°C (Fig. 5F).

Effect of domain structure on thioesterase activity

To assess the contributions of the putative functional domains of Them1 on enzyme activity, we used the truncated Them1 constructs displayed in Fig. 1A. The isolated Thio1 domain exhibited thioesterase activity for myristoyl-CoA and palmitoyl-CoA, albeit with higher K_m and lower V_{max} values compared with Them1 (**Fig. 6**). By doubling the enzyme concentration, the K_m was decreased by 51% and 35% (Fig. 6A), with 20% and 60% increases in V_{max} (Fig. 6B), respectively, for the substrates palmitoyl-CoA and myristoyl-CoA. To further characterize this effect, we measured K_m and V_{max} values for Thio1 compared with Them1 as functions of enzyme concentration using palmitoyl-CoA as the substrate (supplementary Fig. I). At concentrations of Thio1 less than 0.5 µM, we did not detect

enzyme activity. As the Thio1 concentration was increased from 0.5 µM, there was a sharp decline of more than 5-fold in values of K_m, which leveled off starting at 2 µM Thio1 (supplementary Fig. IA). By contrast, there was no concentration dependence of K_m values for Them1, which were similar to the value observed for the highest Thio1 concentration. Over the same range of protein concentrations, there were modest decreases in V_{max} values for Thio1 and little change for Them1 (supplementary Fig. IB).

The recombinant protein Thio1/2, which contained both thioesterase domains, yielded similar K_m and V_{max} values as Thio1 but at half the molar concentration of protein (Fig. 6). We next tested the effect of the START domain of Them1. The START domain alone had no thioesterase activity. However, when added together with Thio1 at a molar ratio of 1:1, the START domain decreased the K_m for palmitoyl-CoA and myristoyl-CoA but increased the V_{max} only for myristoyl-CoA. At a Thio1:START domain molar ratio of 2:1, the START domain further decreased the K_m for both

TABLE 1. Steady-state kinetic constants for Them1-catalyzed hydrolysis of acyl-CoAs.[a]

Acyl-CoA	Protein	K_m (µM)	V_{max}	k_{cat} (s^{-1}) × 10^{-2}	k_{cat}/K_m
			nmol/min/mg		*M/s × 10³*
Arachidonoyl-CoA (C20:4)	Them1	13.3 (3.6)	5.3 (0.4)	1.2	0.9
Stearoyl-CoA (C18:0)		27.9 (4.8)	10.3 (0.8)	2.3	0.8
Oleoyl-CoA (C18:1)		12.8 (4.3)	14.4 (1.2)	3.2	2.5
Linoleoyl-CoA (C18:2)		9.3 (0.5)	12.2 (0.9)	2.7	2.9
Palmitoyl-CoA (C16:0)	Them1	7.5 (0.5)	38.1 (1.8)	8.5	11
	THEM1a	9.1 (0.9)	25.4 (1.2)	5.8	6.4
	THEM1b	7.1 (2.4)	26.5 (0.6)	5.9	8.4
Pamitoleoyl-CoA (C16:1)	Them1	13.6 (2.5)	21 (1.7)	4.7	3.4
Myristoyl-CoA (C14:0)		8.1 (0.9)	20.9 (1.8)	4.7	5.8
Lauroyl-CoA (C12:0)		7.9 (0.9)	23.7 (0.8)	5.3	6.6
Phenylacetyl-CoA		49.8 (8.2)	14.2 (3.3)	3.2	0.6
DL-3-hydroxy-3-methylglutaryl-CoA		86.8 (27.6)	55.9 (17.3)	12	1.4
DL-β-hydroxybutyroyl-CoA		47.9 (5.2)	56.2 (3.9)	13	2.6
2-Butenoyl-CoA		68.2 (1.7)	48.9 (5.6)	11	1.6
Malonyl-CoA		23.2 (2.0)	42.8 (2.9)	9.6	4.1
Acetyl-CoA	Them1	48.1 (3.3)	109 (14.1)	24	5.0
	THEM1a	51.7 (5.1)	78.8 (8.8)	18	3.4
	THEM1b	42.1 (3.5)	108 (12.8)	24	5.7

[a] Reactions were carried out at 37°C using purified recombinant Acots (0.4–0.7 µM). Values of K_m and V_{max} were determined by fitting saturations curves to the Michaelis-Menten equation. The kinetic constants represent means (SEM) of triplicate determinations. We observed slight differences in activity among Them1 preparations, storage time of the protein, and times required for mixing of reagents. To estimate these effects, the kinetic constants were determined on four separate occasions for palmitoyl-CoA. This revealed a variability (1 SD) of 9% for K_m and 10% for V_{max}. Values of k_{cat} were calculated assuming that Them1 was a dimer in solution.
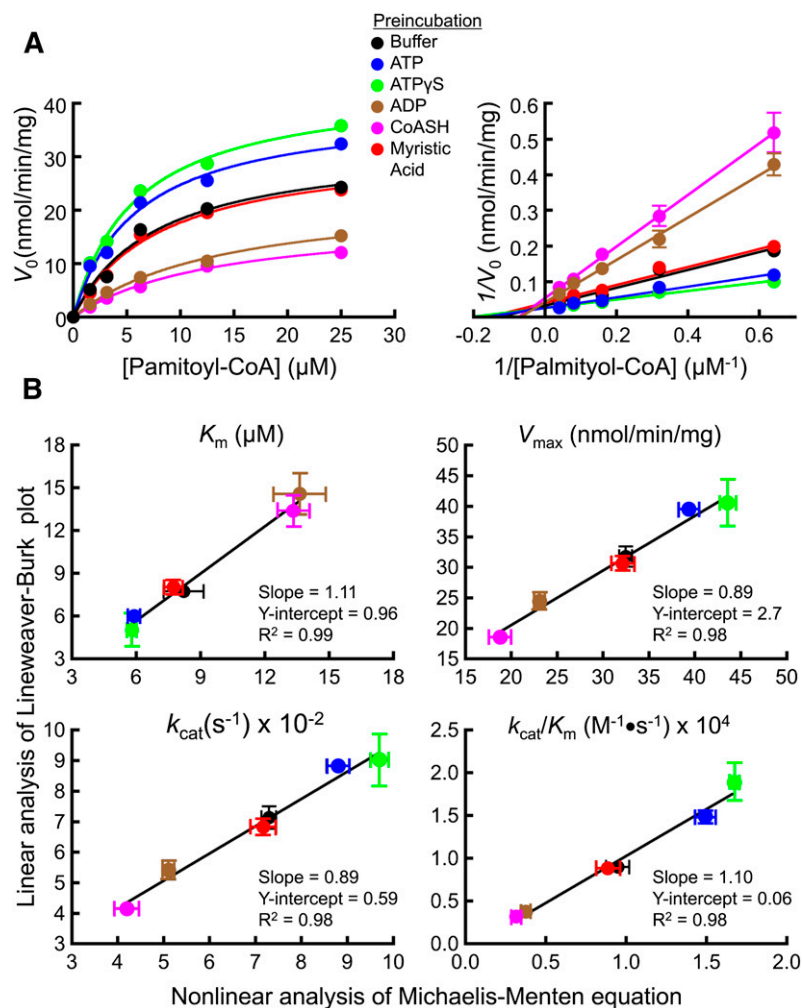
Fig. 4. Influence of small molecules on steady-state kinetic constants for Them1-catalyzed hydrolysis of palmitoyl-CoA. Before measuring values of V_0 at 37°C, Them1 (0.4 μM) was preincubated with ATP (2 mM), ATP-γ-S (0.5 mM), ADP (0.5 mM), CoASH (50 μM), or myristic acid (25 μM) at room temperature for 30 min. A: Saturation curves of V_0 (left panel) and Lineweaver-Burk plots (right panel), with solid lines indicating nonlinear and linear analyses of the data, respectively. To minimize interference by added CoASH in the thioesterase activity assay, Them1 preincubated with CoASH was first ultrafiltered using 10 kDa MWCO Microcon Centrifugal Filter Devices (Millipore). B: Correlations between values of K_m, V_{max}, k_{cat}, and k_{cat}/K_m derived from linear analyses of Lineweaver-Burk plots and nonlinear fits of saturation curves to the Michaelis-Menten equation. Values of k_{cat} were calculated assuming that Them1 was a dimer in solution. Kinetic constants represent triplicate determinations. Where not visible, error bars are contained within the symbol sizes.

fatty acyl-CoAs to near those of intact Them1 and increased values of V_{max}. Similarly, mixing Thio1/2 together with the START domain in a 1:1 molar ratio reduced K_m and increased V_{max} values to very close to intact Them1. Fig. 6 shows that PC-TP lowered K_m values and increased V_{max} values compared with Thio1/2 alone, albeit somewhat more modestly than the START domain of Them1.

Acyl-CoA thioesterase activities of mouse BAT and liver

To assess the contribution of Them1 expression to acyl-CoA thioesterase activity in BAT and liver, we assayed homogenates as well as subcellular fractions isolated from *Them1*^{+/+} and *Them1*^{−/−} mice using palmitoyl-CoA, myristoyl-CoA, and acetyl-CoA as exogenous substrates (**Fig. 7** and supplementary Figs. II and III). Because these preparations contained mixtures of proteins, their acyl-CoA thioesterase activities were characterized as "apparent K_m" and "apparent V_{max}." Homogenates of BAT and liver exhibited thioesterase activity for each substrate. In each tissue, values of apparent K_m for homogenates (Fig. 7 and supplementary Fig. II) were similar to the K_m values of purified recombinant proteins (Table 1). The lack of Them1 expression increased apparent K_m values for each substrate in BAT and liver from 16% to 114%. Values of apparent K_m were generally lower in BAT than in liver

for *Them1*^{+/+} or *Them1*^{−/−} mice. Values of apparent V_{max} were modestly reduced or unchanged in the absence of Them1 expression and were lower in liver compared with BAT from mice of the same genotype.

We next examined the influence of Them1 expression on the acyl-CoA thioesterase activities of subcellular fractions using palmitoyl-CoA (Fig. 7) or acetyl-CoA (supplementary Fig. III) as the exogenous substrate. We previously reported the subcellular distribution of Them1 in wild-type BAT and liver (4). In BAT, Them1 is present in each fraction but is concentrated to the greatest extent in microsomes; in liver, Them1 is mainly cytosolic, with lesser amounts in microsomes, and is barely detectable in mitochondria and nuclei. Values of apparent K_m and apparent V_{max} for cytosol from BAT and liver were close to those observed for tissue homogenates and were similarly influenced by Them1 expression (Fig. 7 and supplementary Fig. III). Apparent K_m values for mitochondrial proteins from BAT were lower than cytosol (Fig. 7A and supplementary Fig. IIIA), and apparent V_{max} values were higher, but these did not vary due to Them1 expression (Fig. 7B and supplementary Fig. IIIB). For microsomes, values of apparent K_m were lower than homogenates and increased in the absence of Them1 expression (Fig. 7A, B and supplementary Fig. IIIA). For BAT, apparent V_{max}
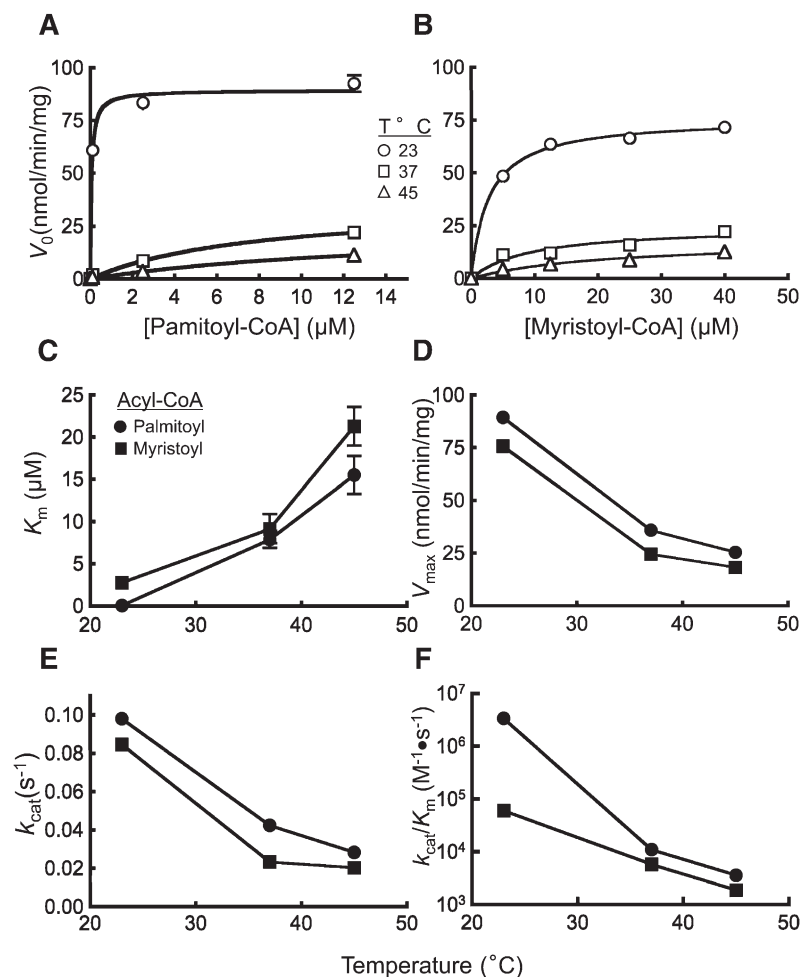
Fig. 5. Temperature dependence of Them1 activity. Saturation curves of V_0 for palmitoyl-CoA (A) and myristoyl-CoA (B) were performed at temperatures ranging from 23°C to 45°C. Solid lines indicate fits of the data to the Michaelis-Menten equation. The influence of temperature on values of the kinetic parameters K_m (C), V_{max} (D), k_{cat} (E), and k_{cat}/K_m (F). Where not visible, error bars are contained within the symbol.

values for palmitoyl-CoA were decreased in microsomes lacking Them1 (Fig. 7C, D) and did not vary in BAT for acetyl-CoA (supplementary Fig. IIIB). For the nuclear fractions from $Them1^{+/+}$ mice, apparent K_m values in BAT and liver were higher than their respective homogenates (Fig. 7A, B). However, no activity was detected in nuclei of BAT or liver harvested from $Them1^{-/-}$ mice (Fig. 7 and supplementary Fig. III). This suggested that Them1 was the major source of fatty acyl-CoA thioesterase activity in nuclei, even though it was expressed there at relatively low levels.

Although the isolated nuclear fractions were determined to be free of other organelle markers (4), we used immunofluorescence (supplementary Fig. IV) and immunohistochemistry (supplementary Fig. V) to confirm nuclear localization. By confocal immunofluorescence microscopy (supplementary Fig. IV), Them1 in BAT was observed to colocalize with a fluorescent nuclear stain in $Them1^{+/+}$ but not $Them1^{-/-}$ mice. Because high levels of autofluorescence from lipid droplets prevented adequate visualization of cytoplasmic Them1 and because immunofluorescence microscopy failed to detect Them1 in liver, we also used immunohistochemistry to image the protein. This revealed nuclear staining, as well as abundant cytoplasmic Them1 in BAT (supplementary Fig. VA) and liver (supplementary Fig. VB) of $Them1^{+/+}$ but not $Them1^{-/-}$ mice.
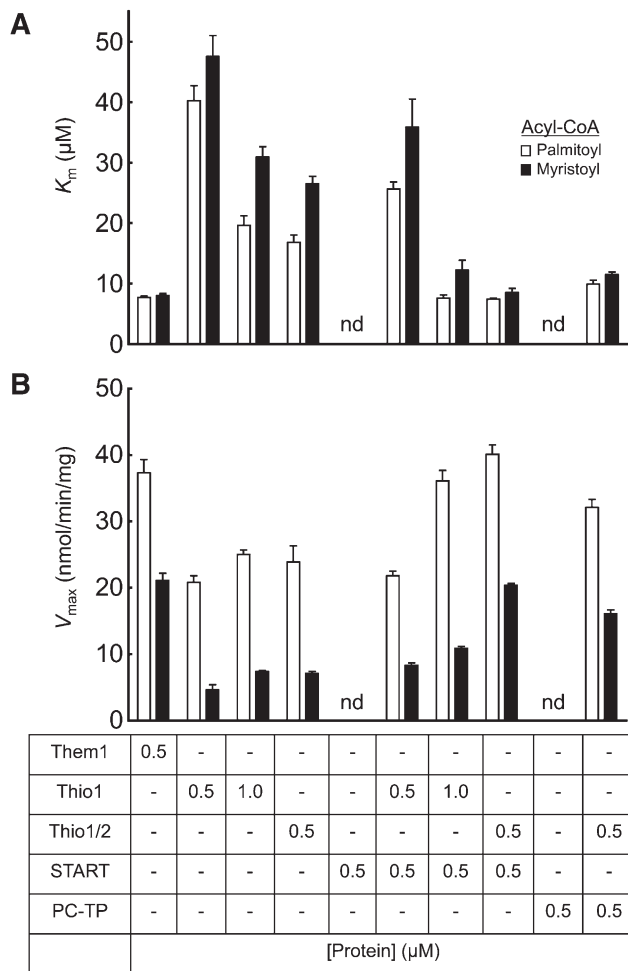
DISCUSSION

Genetic ablation of Them1 in the mouse produced dramatic increases in energy expenditure and improvements in glucose and lipid metabolism (4). To gain insights into regulatory mechanisms, the current study was designed to elucidate biochemical characteristics of Them1.[3] The main findings were that Them1 dimerized to form an Acot with relative preference for long-chain fatty acyl-CoAs and that the START domain optimized enzyme activity. In mouse BAT and liver, loss of Them1 expression had the greatest impact on the acyl-CoA thioesterase activity of the nuclear and microsomal fractions, suggesting cellular functions.

Dimerization of recombinant Them1 is in keeping with other native and recombinant type II Acots for which hot dog-fold domains oligomerize to create active sites that

---

[3]While this manuscript was under consideration, Chen et al. (19) reported that THEM1b (a.k.a. BFIT2), when heterologously expressed in HEK 293T/17 cells or exposed to isolated mitochondria, can be targeted to the mitochondrial matrix and undergo mitochondrion-dependent post-translational cleavage of an N-terminal signal sequence. Whether this occurs to an appreciable extent in vivo is unclear because evidence for cleavage of Them1 in mouse tissues is lacking (4). Although steady-state kinetic constants were not determined for THEM1b, recombinant protein purified from HEK 293T/17 cells exhibited greater thioesterase activity for long chain compared with medium- and shorter-chain fatty acyl-CoAs (19), which is consistent with our findings.

Them1	0.5	-	-	-	-	-	-	-	-	-
Thio1	-	0.5	1.0	-	-	0.5	1.0	-	-	-
Thio1/2	-	-	-	0.5	-	-	-	0.5	-	0.5
START	-	-	-	-	0.5	0.5	0.5	0.5	-	-
PC-TP	-	-	-	-	-	-	-	-	0.5	0.5
[Protein] (µM)										

Fig. 6. Influence of Them1 functional domains on acyl-CoA thioesterase activity. Purified recombinant proteins (see Figure 1A) alone or in combination were preincubated at room temperature for 1 h and then assayed for acyl-CoA thioesterase activities at 37°C using palmitoyl- and myristoyl-CoA as substrates. Saturation curves were fit to the Michaelis-Menten to yield values K_m (A) and V_{max} (B). Protein concentrations are provided in the table below the panels. nd denotes "not detected". Data represent three experiments.

reside at the interfaces between the domains (1, 2). Structural analyses have revealed that the hot dog domains of Acot7 (20), Acot12 (1), Acot13/Them2 (21), Them4 (22), and Acot15/Them5 (23) form dimers or oligomers of dimers. However, these structures are not uniformly representative of the enzymes in solution. For example, Acot12 functions as a dimer and a tetramer in solution (24) even though the crystal structure of its thioesterase domains reveals a trimer of hot dog-fold dimers (1). This apparent discrepancy could reflect the influence of the START domain on oligomerization of Acot12.

The balance between Acot12 dimers and tetramers depends upon enzyme concentration and temperature and on the presence of acetyl-CoA, ATP, and ADP (24). As functions of decreasing temperature to 4°C, Acot12 oligomers dissociate into monomers and lose activity (25). Indicative of its role in oligomerization, acetyl-CoA inhibits cold inactivation of Acot12 (24) and facilitates reactivation of the enzyme upon warming (17). Our finding that

acetyl-CoA promotes Acot12 tetramer formation is in accordance with these observations. Although temperature per se did not influence oligomerization of Them1, its dimerization was effected by the presence of a fatty acyl-CoA. Collectively, these findings demonstrate that the substrates of Acot12 and Them1 mediate oligomerization. ATP promotes tetramerization of Acot12 (25) and its activation (18). Here we showed that it also induced dimerization and increased activity for Them1. Like Acot12 (18), ATP hydrolysis was not required for the activation of Them1, as evidenced by similar effects of ATP and ATP-γ-S on oligomerization and enzymatic activity. ADP induced Them1 to dimerize yet decreased its activity. This is in keeping with the observation that ADP promotes tetramerization of Acot12 while at the same inactivating the enzyme (26). The effects of ATP and ADP on Acot12 were attributed to the potential presence of a nucleotide binding site in proximity to the enzyme active site (26). Because nucleotide effects on Acot12 activity were consistent with simple competitive displacements, it was concluded that ATP and ADP more likely induce conformational changes that lead to different catalytic activities and substrate affinities. Consistent with this possibility for Them1, Lineweaver-Burk plots were indicative of a mixed mechanism of inhibition. The mechanism by which CoASH inhibits Acot12 (18) and Them1 is not known but may be due to the presence of ADP within its molecular structure.

With the exception of Acot12, medium- and long-chain acyl-CoAs are generally the preferred substrates of type II Acots (1), an observation that extends to the more recently characterized Them4 (22) and Them5/Acot15 (23). Although previously suggested to hydrolyze medium- and long-chain fatty acyl-CoAs (9), in the current study Them1 cleaved a range of substrates, albeit demonstrating a relative preference for medium- to long-chain fatty acyl-CoAs. The steady-state kinetic constants for fatty acyl-CoA hydrolysis for Them1 fall in similar ranges as those of Them2 (8), Them4 (22), and Them5 (23). When characterized using a short- and a long-chain fatty acyl-CoA substrate, THEM1a and THEM1b yielded similar kinetic constants as Them1, suggesting that the additional 13 aa at the C terminus of THEM1a (9) serves a function separate from the enzymatic activity of the protein.

The intracellular concentrations of fatty acyl-CoAs remain an important unresolved issue in understanding the biologic functions of Acots. Total intracellular concentrations of long-chain fatty acyl-CoAs range from 5 µM in neutrophils to 164 µM in liver (27), with estimates of 30–90 µM in cytosol, 0.2–3.1 mM in mitochondria, and 0.4 mM in peroxisomes (2). This suggests 25 µM palmitoyl-CoA, which we used in our oligomerization studies, should fall within the biological range. Such intracellular fatty acyl-CoA concentrations would also be in keeping with the K_m values we observed for Them1 and with those reported for other Acots (8, 22, 23, 28). However, fatty acyl-CoAs may bind to proteins and cell membranes, and this would presumably reduce their accessibility to Acots. Although the unbound fatty acyl-CoA concentrations in cells are not known, estimates ranging from 1 to 200 nM have been
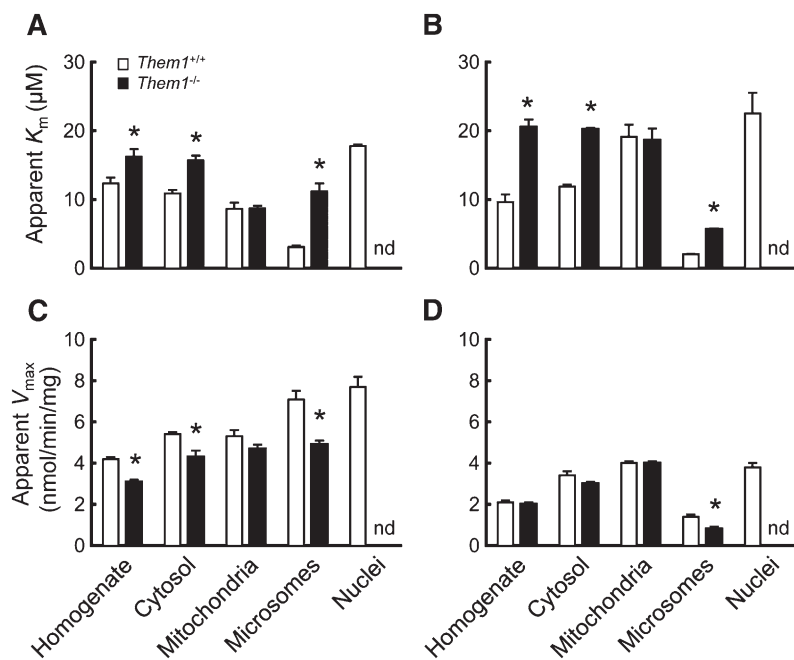
Fig. 7. Influence of Them1 expression on palmitoyl-CoA thioesterase activity in BAT and liver. Homogenates and subcellular fractions (50 μg) from BAT (A, C) and livers (B, D) of $Them1^{+/+}$ and $Them1^{-/-}$ mice were assayed at 37°C using palmitoyl-CoA as an exogenous substrate. Saturation curves were fit to the Michaelis-Menten equation to determine values of apparent K_m (A, B) and apparent V_{max} (C, D). Data points represent triplicate determinations. * $P < 0.05$.

based on the affinities of acyl-CoA binding proteins and on partition coefficients of acyl-CoAs into cell membranes (27). If this is true, then unbound fatty acyl-CoAs would exist within cells at concentrations that are far below the observed K_m values for Acots. They would also fall far below the micromolar ranges of concentrations at which long-chain fatty acyl-CoAs have been observed in numerous studies to regulate cellular biological processes, including lipid metabolism, energy homeostasis, and signal transduction (27). Additional study is required to resolve these issues.

The responses of Them1 activity to increases in temperature were qualitatively similar to effects observed for Them2 (8) but more pronounced in magnitude. Because the temperature at which Them2 tetramers became dissociated and unfolded was close to 60°C, it was unlikely a loss of hot dog-fold structure was responsible for the sharp decline in k_{cat}/K_m that occurred for Them1 between 25°C and 37°C. This could instead reflect dissociation of Them1 dimers or reduced binding of the hydrophobic substrate to the enzyme. The latter possibility is supported by the sharper decline in k_{cat}/K_m observed for palmitoyl-CoA than for myristoyl-CoA. Considering that the changes in Them1 activity were more modest when the temperature was raised to 45°C, a physiological significance of this thermal effect is uncertain. In this connection, the tissue temperature of BAT has been shown to increase in response to norepinephrine stimulus (29), but the change was only ∼3°C.

The functional interactions between PC-TP and Them2 (7, 8) prompted us to examine the roles of the individual thioesterase domains and the START domain in determining the acyl-CoA thioesterase activity. Our kinetic analysis revealed that the presence of these domains within a single protein was not required to optimize enzyme activity. The isolated N-terminal Thio1 domain of Them1 yielded long-chain fatty acyl-CoA thioesterase activity of the same extent as the Thio1/2 tandem thioesterase domains, provided

that the domains were present in the same molar concentration. The concentration-dependent enzymatic characteristics of Thio1 strongly suggest that the aggregative states of this specific hot dog-fold domain dictate overall activity, a phenomenon not observed for the intact Them1 protein. By contrast, Acot7 comprises tandem thioesterase domains, and both domains are required for activity (20). Individually, the two thioesterases exhibited no significant activity, but activity was restored when the two were combined. The Them1 START domain also made important contributions toward optimizing the acyl-CoA thioesterase activity. We previously reported that recombinant PC-TP maximized Them2 activity at a molar ratio of PC-TP:Them2 of 1:2 (7). The current findings indicate that the Them1 START domain restored K_m and V_{max} values close to those of intact Them1, provided that the START domain and thioesterase domains were also in a 1:2 molar ratio. This occurred irrespective of whether the START domain was mixed with Thio1 or Thio1/2. When taken together with the observation that PC-TP could effectively substitute for the Them1 START domain, these findings argue against the likelihood that these protein domains are incorporated into a single protein to facilitate enzyme activity. Instead, this may permit the domains to be selectively colocalized within the cell. By contrast, PC-TP and Them2 are individually targeted to mitochondria ,where they engage in interactions. Whereas Them2 is enriched in mitochondria (8), PC-TP is enriched in cytosol but relocalizes to mitochondria in response to selective cell signaling events (30).

An important limitation of our experiments is that they did not assess the influence of the endogenous ligand of Them1, which is currently unknown. It has been postulated that START domains within multidomain proteins may function as lipid sensors (6), whereby binding of the lipid regulates the activity of the other domains (5). Although the crystal structure of the Them1 START domain has

revealed a characteristic lipid binding pocket (31), there was no lipid ligand present after its recombinant expression in *E. coli*, purification, and crystallization. As with the influence of PC-TP on Them2 activity (32), it will be important to define the influence of ligand binding on the activity of Them1.

The enzymatic analysis of subcellular fractions of BAT and liver from *Them1*$^{-/-}$ and *Them1*$^{+/+}$ mice offers some potential insights into the contributions of Them1 to the knockout mouse phenotypes. The absence of Them1 expression attenuated cellular responses to diet- and chemically induced endoplasmic reticulum (ER) stress (4). This was postulated to be due to reduced production of free fatty acids under conditions that promote ER stress. The measurable contribution of Them1 to acyl-CoA thioesterase activity in microsomes and cytosol is consistent with this possibility. Although present, Them1 was not enriched in nuclei (4). Therefore, we did not anticipate that the absence of acyl-CoA thioesterase activity would be observed in nuclei isolated from BAT and liver of *Them1*$^{-/-}$ mice. Although we cannot exclude relocalization of other Acots away from nuclei in response to genetic ablation of Them1, the mRNA levels encoding other Acot genes were largely increased in BAT of *Them1*$^{-/-}$ mice. Assuming that Them1 does contribute substantially to the acyl-CoA thioesterase activity in the nucleus, this finding suggests a potential role in controlling the relative concentrations of acyl-CoAs and free fatty acids that serve as ligands for the nuclear receptors hepatocyte nuclear factor 4α and peroxisome proliferator-activated receptor α (32). Considering its physiological role in limiting fatty acid oxidation, it is also noteworthy that the absence of Them1 did not influence the acyl-CoA thioesterase activity associated with mitochondria in BAT or liver.⬛⬛

REFERENCES

1. Kirkby, B., N. Roman, B. Kobe, S. Kellie, and J. K. Forwood. 2010. Functional and structural properties of mammalian acyl-coenzyme A thioesterases. *Prog. Lipid Res.* **49:** 366–377.
2. Hunt, M. C., and S. E. Alexson. 2002. The role Acyl-CoA thioesterases play in mediating intracellular lipid metabolism. *Prog. Lipid Res.* **41:** 99–130.
3. Kang, H. W., M. W. Niepel, S. Han, Y. Kawano, and D. E. Cohen. 2012. Thioesterase superfamily member 2/acyl-CoA thioesterase 13 (Them2/Acot13) regulates hepatic lipid and glucose metabolism. *FASEB J.* **26:** 2209–2221.
4. Zhang, Y., Y. Li, M. W. Niepel, Y. Kawano, S. Han, S. Liu, A. Marsili, P. R. Larsen, C. H. Lee, and D. E. Cohen. 2012. Targeted deletion of thioesterase superfamily member 1 promotes energy expenditure and protects against obesity and insulin resistance. *Proc. Natl. Acad. Sci. USA.* **109:** 5417–5422.
5. Schrick, K., D. Nguyen, W. M. Karlowski, and K. F. Mayer. 2004. START lipid/sterol-binding domains are amplified in plants and are predominantly associated with homeodomain transcription factors. *Genome Biol.* **5:** R41.
6. Alpy, F., and C. Tomasetto. 2005. Give lipids a START: the StAR-related lipid transfer (START) domain in mammals. *J. Cell Sci.* **118:** 2791–2801.
7. Kanno, K., M. K. Wu, D. A. Agate, B. K. Fanelli, N. Wagle, E. F. Scapa, C. Ukomadu, and D. E. Cohen. 2007. Interacting proteins dictate function of the minimal START domain phosphatidylcholine transfer protein/StarD2. *J. Biol. Chem.* **282:** 30728–30736.
8. Wei, J., H. W. Kang, and D. E. Cohen. 2009. Thioesterase superfamily member 2 (Them2)/acyl-CoA thioesterase 13 (Acot13): a homotetrameric hotdog fold thioesterase with selectivity for long-chain fatty acyl-CoAs. *Biochem. J.* **421:** 311–322.
9. Adams, S. H., C. Chui, S. L. Schilbach, X. X. Yu, A. D. Goddard, J. C. Grimaldi, J. Lee, P. Dowd, S. Colman, and D. A. Lewin. 2001. BFIT, a unique acyl-CoA thioesterase induced in thermogenic brown adipose tissue: cloning, organization of the human gene and assessment of a potential link to obesity. *Biochem. J.* **360:** 135–142.
10. Feng, L., W. W. Chan, S. L. Roderick, and D. E. Cohen. 2000. High-level expression and mutagenesis of recombinant human phosphatidylcholine transfer protein using a synthetic gene: evidence for a C-terminal membrane binding domain. *Biochemistry.* **39:** 15399–15409.
11. Corrin, M. L., H. B. Klevens, and W. D. Harkins. 1946. The determination of critical concentrations for the formation of soap micelles by the spectral behavior of pinacyanol chloride. *J. Chem. Phys.* **14:** 480–486.
12. Cox, B., and A. Emili. 2006. Tissue subcellular fractionation and protein extraction for use in mass-spectrometry-based proteomics. *Nat. Protoc.* **1:** 1872–1878.
13. Smith, R. H., and G. L. Powell. 1986. The critical micelle concentration of some physiologically important fatty acyl-coenzyme A's as a function of chain length. *Arch. Biochem. Biophys.* **244:** 357–360.
14. Constantinides, P. P., and J. M. Steim. 1985. Physical properties of fatty acyl-CoA. Critical micelle concentrations and micellar size and shape. *J. Biol. Chem.* **260:** 7573–7580.
15. Powell, G. L., J. R. Grothusen, J. K. Zimmerman, C. A. Evans, and W. W. Fish. 1981. A re-examination of some properties of fatty acyl-CoA micelles. *J. Biol. Chem.* **256:** 12740–12747.
16. Constantinides, P. P., and J. M. Steim. 1988. Micellization of fatty acyl-CoA mixtures and its relevance to the fatty acyl selectivity of acyltransferases. *Arch. Biochem. Biophys.* **261:** 430–436.
17. Isohashi, F., Y. Nakanishi, T. Matsunaga, and Y. Sakamoto. 1984. A cold-labile acetyl-coenzyme-A hydrolase from the supernatant fraction of rat liver. Reactivation and reconstitution of the active species from the inactive monomer. *Eur. J. Biochem.* **142:** 177–181.
18. Prass, R. L., F. Isohashi, and M. F. Utter. 1980. Purification and characterization of an extramitochondrial acetyl coenzyme A hydrolase from rat liver. *J. Biol. Chem.* **255:** 5215–5223.
19. Chen, D., J. Latham, H. Zhao, M. Bisoffi, J. Farelli, and D. Dunaway-Mariano. 2012. Human brown fat inducible thioesterase variant 2 cellular localization and catalytic function. *Biochemistry.* **51:** 6990–6999.
20. Forwood, J. K., A. S. Thakur, G. Guncar, M. Marfori, D. Mouradov, W. Meng, J. Robinson, T. Huber, S. Kellie, J. L. Martin, et al. 2007. Structural basis for recruitment of tandem hotdog domains in acyl-CoA thioesterase 7 and its role in inflammation. *Proc. Natl. Acad. Sci. USA.* **104:** 10382–10387.
21. Cheng, Z., F. Song, X. Shan, Z. Wei, Y. Wang, D. Dunaway-Mariano, and W. Gong. 2006. Crystal structure of human thioesterase superfamily member 2. *Biochem. Biophys. Res. Commun.* **349:** 172–177.
22. Zhao, H., B. M. Martin, M. Bisoffi, and D. Dunaway-Mariano. 2009. The Akt C-terminal modulator protein is an acyl-CoA thioesterase of the Hotdog-Fold family. *Biochemistry.* **48:** 5507–5509.
23. Zhuravleva, E., H. Gut, D. Hynx, D. Marcellin, C. K. Bleck, C. Genoud, P. Cron, J. J. Keusch, B. Dummler, M. D. Esposti, et al. 2012. Acyl-CoA thioesterase Them5/Acot15 is involved in cardiolipin remodeling and fatty liver development. *Mol. Cell. Biol.* **32:** 2685–2697.
24. Isohashi, F., Y. Nakanishi, and Y. Sakamoto. 1983. Factors affecting the cold inactivation of an acetyl-coenzyme-A hydrolase purified from the supernatant fraction of rat liver. *Eur. J. Biochem.* **134:** 447–452.
25. Isohashi, F., Y. Nakanishi, and Y. Sakamoto. 1983. Effects of nucleotides on a cold labile acetyl-CoA hydrolase from the supernatant fraction of rat liver. *Biochemistry.* **22:** 584–590.
26. Nakanishi, Y., F. Isohashi, S. Ebisuno, and Y. Sakamoto. 1988. Binding of nucleotides to an extramitochondrial acetyl-CoA hydrolase from rat liver. *Biochemistry.* **27:** 4822–4826.
27. Knudsen, J., M. V. Jensen, J. K. Hansen, N. J. Faergeman, T. B. Neergaard, and B. Gaigg. 1999. Role of acylCoA binding protein in acylCoA transport, metabolism and cell signaling. *Mol. Cell. Biochem.* **192:** 95–103.

28. Cao, J., H. Xu, H. Zhao, W. Gong, and D. Dunaway-Mariano. 2009. The mechanisms of human hotdog-fold Thioesterase 2 (hTHEM2) substrate recognition and catalysis illuminated by a structure and function based analysis. *Biochemistry*. **48:** 1293–1304.

29. Ribeiro, M. O., S. D. Carvalho, J. J. Schultz, G. Chiellini, T. S. Scanlan, A. C. Bianco, and G. A. Brent. 2001. Thyroid hormone–sympathetic interaction and adaptive thermogenesis are thyroid hormone receptor isoform–specific. *J. Clin. Invest.* **108:** 97–105.

30. de Brouwer, A. P., J. Westerman, A. Kleinnijenhuis, L. E. Bevers, B. Roelofsen, and K. W. A. Wirtz. 2002. Clofibrate-induced relocation of phosphatidylcholine transfer protein to mitochondria in endothelial cells. *Exp. Cell Res.* **274:** 100–111.

31. Thorsell, A. G., W. H. Lee, C. Persson, M. I. Siponen, M. Nilsson, R. D. Busam, T. Kotenyova, H. Schuler, and L. Lehtio. 2011. Comparative structural analysis of lipid binding START domains. *PLoS ONE.* **6:** e19521.

32. Kang, H. W., J. Wei, and D. E. Cohen. 2010. PC-TP/StARD2: of membranes and metabolism. *Trends Endocrinol. Metab.* **21:** 449–456.